

Journal Pre-proof

Formation of metal-organic ligand complexes affects solubility of metals in airborne particles at an urban site in the Po valley

Andrea Tapparo, Valerio Di Marco, Denis Badocco, Sara D'Aronco, Lidia Soldà, Paolo Pastore, Brendan M. Mahon, Markus Kalberer, Chiara Giorio



PII: S0045-6535(19)32264-7

DOI: <https://doi.org/10.1016/j.chemosphere.2019.125025>

Reference: CHEM 125025

To appear in: *ECSN*

Received Date: 14 July 2019

Revised Date: 28 September 2019

Accepted Date: 30 September 2019

Please cite this article as: Tapparo, A., Di Marco, V., Badocco, D., D'Aronco, S., Soldà, L., Pastore, P., Mahon, B.M., Kalberer, M., Giorio, C., Formation of metal-organic ligand complexes affects solubility of metals in airborne particles at an urban site in the Po valley, *Chemosphere* (2019), doi: <https://doi.org/10.1016/j.chemosphere.2019.125025>.

This is a PDF file of an article that has undergone enhancements after acceptance, such as the addition of a cover page and metadata, and formatting for readability, but it is not yet the definitive version of record. This version will undergo additional copyediting, typesetting and review before it is published in its final form, but we are providing this version to give early visibility of the article. Please note that, during the production process, errors may be discovered which could affect the content, and all legal disclaimers that apply to the journal pertain.

© 2019 Published by Elsevier Ltd.

Formation of metal-organic ligand complexes affects solubility of metals in airborne particles at an urban site in the Po Valley

Andrea Tapparo¹, Valerio Di Marco¹, Denis Badocco¹, Sara D'Aronco¹, Lidia Soldà¹, Paolo Pastore¹,
Brendan M. Mahon², Markus Kalberer^{2,3}, and Chiara Giorio^{1,2*}

¹ Department of Chemical Sciences, University of Padua, via Marzolo 1, 35131 Padova, Italy

² Department of Chemistry, University of Cambridge, Lensfield Road, Cambridge, CB2 1EW, United Kingdom

³ Department of Environmental Sciences, University of Basel, Klingelbergstrasse 27, 4056 Basel, Switzerland

* Corresponding author: chiara.giorio@unipd.it

Abstract

Metals in atmospheric aerosols play potentially an important role in human health and ocean primary productivity. However, the lack of knowledge about solubility and speciation of metal ions in the particles or after solubilisation in aqueous media (sea or surface waters, cloud or rain droplets, biological fluids) limits our understanding of the underlying physico-chemical processes. In this work, a wide range of metals, their soluble fractions, and inorganic/organic compounds contained in urban particulate matter (PM) from Padua (Italy) were determined. Metal solubility tests have been performed by dissolving the PM in water and in solutions simulating rain droplet composition. The water-soluble fractions of the metal ions and of the organic compounds having ligand properties have been subjected to a multivariate statistical procedure, in order to elucidate associations among the aqueous concentrations of these PM components in simulated rain droplets. In parallel, a multi-dimensional speciation calculation has been performed to identify the stoichiometry and the amount of metal-ligand complexes theoretically expected in aqueous solutions. Both approaches showed that the solubility and the aqueous speciation of metal ions were differently affected by the presence of inorganic and organic ligands in the PM. The solubility of Al, Cr, and Fe was strongly correlated to the concentrations of oxalic acid, as their oxalate complexes represented the expected dominant species in aqueous solutions. Oxalates of Al represented ~98% of soluble Al, while oxalates of Cu represented 34-75% of the soluble Cu, and oxalates of Fe represented 76% of soluble Fe. The oxidation state of Fe can strongly impact the speciation picture. If Fe is present as Fe(II) rather than Fe(III), the amount of Cr and Cu complexed with diacids can increase from 75% to 94%, and from 32% to 53%, respectively. For other metals, the solubility depended on the formation of soluble aquo-complexes, hence with a scarce effect of the organic ligands. An iron-oxalate complex was also directly detected in aerosol sample extracts.

35 **Keywords**

36 Metal-ligand complexes; deliquescent aerosol; urban PM_{2.5}; oxalate; iron

Journal Pre-proof

37 1. Introduction

38 Despite air quality policies established worldwide, the progress in reducing airborne
39 particulate matter (PM) has been slow in recent years and PM still remains one of the major
40 polluting agents in the urban atmosphere, posing a substantial burden for public health (Harrison et
41 al., 2010; Lelieveld et al., 2019; Raaschou-Nielsen et al., 2013; Shiraiwa et al., 2017). According to
42 WHO about 90% of the world's population live in areas with unhealthy air, leading to increased
43 mortality and morbidity (WHO, 2016). Air pollution contributes to total mortality more than
44 malaria and HIV combined on a global scale (Lelieveld et al., 2015) and represents the largest
45 environmental risk factor behind premature deaths (Burnett et al., 2018).

46 The majority of epidemiological studies have used particulate mass (PM_{10} or $PM_{2.5}$) as the
47 metric of choice, largely because of the availability of monitoring data. However, this approach is
48 considered incomplete and can lead to an underestimation of PM risk (Harrison et al., 2010).
49 Despite toxicological studies have shown that chemical composition may play an important role in
50 $PM_{2.5}$ -induced toxicity (Perrone et al., 2010), the chemical species responsible for PM toxicological
51 properties remain a subject of investigation (Decesari et al., 2017). The adverse health effects of
52 $PM_{2.5}$ can be ascribed to polycyclic aromatic hydrocarbons (PAHs) and their nitrated or oxygenated
53 (e.g. quinones) derivatives (Giorio et al., 2019a), the primary biogenic fraction, such as pathogenic
54 bacteria and bacterial endotoxins (Franzetti et al., 2011; Topinka et al., 2011), and water soluble PM
55 fractions such as water soluble organic (WSOC) and inorganic compounds, and metal ions like Zn,
56 Pb and Ni (Birmili et al., 2006; Chen and Lippmann, 2009; Oberdörster et al., 2005; Zhang et al.,
57 2015). The toxic effects caused by Al, Fe and Cu can be also important, as these ions represent the
58 major metal components in PM arising from different sources (Deguillaume et al., 2005).

59 The bioavailability, rather than the total concentration, of pollutants released by PM in water,
60 as it occurs on the lung surface after inhalation, is expected to correlate with the observed toxic
61 effects. In turn, the bioavailability of each compound strongly depends on its chemical speciation,
62 i.e. on the chemical form by which it is dissolved in solution. As many WSOC and inorganic
63 compounds have coordinating properties towards metal ions, bioavailability depends on the
64 stoichiometry and stability constants of the complexes formed in solution between the metal ions
65 and the ligands contained in PM, after PM enters into contact with water (Giorio et al., 2017;
66 Scheinhardt et al., 2013; Wei et al., 2019). Therefore, a more complete risk assessment of PM
67 requires not only the knowledge of the total concentration of all compounds contained in PM, but
68 also of the stoichiometry of the metal-ligand complexes formed, and of their concentration. This
69 "speciation" approach has been introduced in a fundamental review by Okochi and Brimblecombe,
70 (2002). However, detailed investigations on this topic are scarce. The majority of the studies relate

71 the speciation of the PM metal ions with ligands already present in the environment (marine
72 environment or surface waters), whereas only very few studies consider ligands present in the
73 aerosol particles themselves (DePalma et al., 2011; Elzinga et al., 2011; Jickells et al., 2005; Paris et
74 al., 2011; Paris and Desboeufs, 2013; Schroth et al., 2009; Wang et al., 2007). A study from
75 Scheinhardt et al. (2013) suggested that metal-ligand interactions may be an important phenomenon
76 in deliquescent aerosol in the urban atmosphere. As the particles travel deeper into the respiratory
77 system, consisting of wet walled respiratory tracts, they encounter increasing humidity: ~40% in the
78 mouth, ~60% in the pharynx, to finally approaching near water saturation ~99.5% in the deep
79 airways. Hygroscopic particles moving from a region of low ambient humidity into one of high
80 humidity would be expected to increase in size due to water uptake and this will favour
81 coordination chemistry (Tong et al., 2014).

82 The northern Italian Po Valley, a semi-closed basin surrounded by complex orography,
83 represents a natural laboratory for studying aqueous phase processing of aerosol. It is one of the
84 major European air pollution hotspots and environmental conditions favour fog events during the
85 winter. In this work, an urban PM (Padua, Italy) was subjected to a chemical characterization in
86 order to identify and quantify the most relevant metal ions and inorganic/organic compounds. Metal
87 content has been determined by inductively coupled plasma mass spectrometry (ICP-MS), whereas
88 organic/inorganic ligands have been measured by ion chromatography (IC). Metal solubility tests
89 have been performed by dissolving the PM in water and in solutions simulating fog/rain
90 composition. The water-soluble fractions of the metal ions and of the inorganic/organic compounds
91 having ligand properties have been subjected to a multivariate statistical procedure. In parallel, a
92 multi-dimensional speciation calculation has been performed to evaluate the stoichiometry and the
93 concentrations of metal-ligand complexes expected in aqueous solutions. For those complexes
94 expected at higher concentrations their detection was also attempted by nano electrospray ionisation
95 high-resolution mass spectrometry (nanoESI-HRMS) investigations.

96

97 **2. Experimental**

98 **2.1. Chemicals and standard solutions**

99 All reagents were of analytical grade and were used as purchased: 69 % HNO₃ (PROLABO,
100 Milan, Italy), multi-element standard solution IV-ICPMS-71A (10 mg L⁻¹) ICP-MS calibration
101 standard (Inorganic Ventures, Christiansburg, VA 24073 USA). All solutions were prepared in
102 ultrapure water obtained with a Millipore Plus System (Milan, Italy, resistivity 18.2 Ω cm⁻¹).

103 Primary standards for IC analysis were of analytical grade and purchased from Sigma-
104 Aldrich®. Methanol (Optima™ LC/MS, Fisher Chemical) was used for washing and sample
105 extraction for nanoESI-HRMS analysis.

106 **2.2. Aerosol sampling**

107 Teflon filters (PALL, fiberfilm, Ø 47 mm) were pre-washed with large amounts (~250 mL for
108 all filters used) of ultrapure water for three times under ultrasonic agitation for 15 mins, changing
109 water each time. Quartz fibre filters (Millipore, AQFA, Ø 47 mm) were decontaminated by baking
110 them at 600 °C for 24 h.

111 PM_{2.5} samples were collected (sampling time 24 h, from 00.00 to 24.00) at the sampling site
112 located at the 6th floor of the Department of Chemical Sciences of the University of Padova (Italy),
113 using a Zambelli Explorer Plus PM sampler, fitted with a PM_{2.5} certified selector (CEN standard
114 method UNI-EN 14907), and working at a constant flow rate of 2.3 m³ h⁻¹ (Giorio et al., 2013) from
115 the 5th December 2013 to the 1st April 2014, alternating Teflon and quartz filters (see Table S1 in
116 the supplementary material for details).

117 Weighing of the filters was done for Teflon filters only, before and after sampling, after
118 conditioning at a temperature of 20 ± 1 °C and relative humidity of 50 ± 5% for at least 48 h, as in
119 previous studies (Giorio et al., 2013, 2019b). Filter samples were then stored at -20°C until analysis.

120 **2.3. Sample Preparation**

121 Teflon filters were manually cut into three parts (two parts of ¼ and one part of ½) by a
122 stainless-steel cutter. The use of a stainless-steel cutter did not cause contaminations for the metal
123 determination, as checked by analysis of procedural blanks. For each sample, ¼ filter was treated
124 with 2 mL of 69% nitric acid using a CEM Discover SP-D (CEM Corp., Matthews, NC, USA)
125 microwave digester at 400 psi and 300 W, with a temperature ramp from 20 °C to 200 °C in 4 min,
126 and maintained at the final conditions for 2 min. The solution was diluted to 3.45 % w/w nitric acid
127 before analysis by ICP-MS. Another ¼ filter was extracted in 5 mL of a pH 4.5 water solution of
128 H₂SO₄ at 20°C, simulating fog/rainwater (Beiderwieden et al., 2005; Nieberding et al., 2018; Rodhe
129 et al., 2002; Walna, 2015; Wang et al., 2012), for 24h without stirring. After that, 4 mL of solution
130 were taken and concentrated HNO₃ (69%) was added to obtain a concentration of 3.45 % (w/w)
131 HNO₃ for ICP-MS analysis. Another ½ filter was extracted in 5 mL of ultrapure water at 20°C for
132 24h without stirring. After that, 2 mL were taken and filtered with 0.45 µm syringe filters (Millex®-
133 HV, PVDF, Ø 4 mm) before IC analysis. The other 3 mL were taken, and concentrated HNO₃ was
134 added to obtain a concentration of 3.45 % (w/w) HNO₃ for ICP-MS analysis.

135 Quartz fibre filters were extracted according to the procedure already described elsewhere
136 (Kourtchev et al., 2014) before analysis with nanoESI-HRMS. For each filter sample, the outer ring

137 of the filter, which had been in contact with the filter holder during sample collection, was removed
138 to prevent contamination and a portion of the filter (the whole filter in the case of blanks and $\frac{1}{4}$ in
139 all other cases) was cut into small (*ca.* 25-100 mm²) pieces and placed in a glass vial. The pieces of
140 quartz filter were then covered with 5 mL of methanol and extracted by ultrasonic agitation for 30
141 minutes in slurry ice. The resulting methanol extracts were then transferred to a new pre-cleaned
142 vial and concentrated via evaporation under a gentle stream of nitrogen (BOC, Guildford, UK) to
143 *ca.* 2 mL on a hotplate (SD160, Stuart, Stone, UK), which was kept at 35°C. The concentrated
144 extracts were filtered through two syringe PTFE filters (ISO-Disc™, Supelco, with pore sizes of
145 0.45 μm and 0.22 μm). The filtered extracts were then concentrated further, by evaporation under a
146 gentle stream of nitrogen, to *ca.* 0.1 mL and kept in a washed glass vial at -20° in darkness until
147 analysis.

148 For each analysis type, procedural blanks (unexposed filters) were also obtained and
149 analysed.

150

151 **2.4. Instrumental Analysis**

152 **2.4.1. Analysis of metals with ICP-MS**

153 All elements were determined by using an ICP-MS (Agilent 7700x, Agilent Technologies,
154 Santa Clara, CA, USA). The operating conditions and data acquisition parameters are reported in
155 previous studies (Badocco et al., 2014; Giorio et al., 2019b). The ICP-MS was tuned daily using a
156 1 $\mu\text{g L}^{-1}$ tuning solution containing ¹⁴⁰Ce, ⁵⁹Co, ⁷Li, ²⁰⁵Tl and ⁸⁹Y (Agilent Technologies, UK). The
157 ratio 156/140 representing CeO/Ce is tuned to approximately 1% or less. The ratio 70/140
158 representing Ce²⁺/Ce is maintained below 3%. A 50 $\mu\text{g L}^{-1}$ solution of ⁴⁵Sc and ¹¹⁵In (Aristar®,
159 BDH, UK) prepared in 3.45 % (w/w) nitric acid was used as an internal standard through addition
160 to the sample solution via a T-junction.

161 Multielement standard solutions were prepared in 3.45 % w/w HNO₃. The calibration
162 solutions were prepared by gravimetric serial dilution from multi-element standard solutions in the
163 range between 1 ng L⁻¹ and 1 mg L⁻¹. The detection limit of each element was determined using five
164 concentration levels replicated nine times. Blank samples of ultrapure water and reagents were also
165 prepared using the same procedures adopted for the samples.

166 **2.4.2. Analysis of soluble inorganic anions and short-chain organic acids**

167 Instrumental analysis was performed by injecting 20 μL of water extracts in a Dionex IC
168 system equipped with an a GP50 Gradient Pump, an EG40 eluent generation system fitted with a
169 Dionex EGC III KOH RFIC™ eluent generator cartridge, a LC25 oven, and an ED40
170 Electrochemical Detector (in conductometric detection mode), and fitted with a Dionex IonPac

171 AG11-HC (2 x 50 mm) guard column, a Dionex IonPac AS11-HC (2 x 250 mm) chromatographic
172 column, and a Dionex AERS 500 (2 mm) self-regenerating suppressor (suppression current
173 100 mA). Chromatographic separation was achieved at room temperature (~20 °C), with a flow rate
174 of 300 µL/min, and elution gradient: 0–3 min 3 mM KOH, 3-5 min linear gradient from 3 mM to
175 10 mM KOH, 5-12 min linear gradient from 10 mM to 20 mM KOH, 12-20 min 20 mM KOH,
176 20-24 min linear gradient from 20 mM to 40 mM KOH and 24-35 min 40 mM KOH. Equilibration
177 time at the beginning of each chromatographic run was 7 min.

178 External calibration was performed daily with standard solutions in the range 0.1–50 mg/L of
179 each analyte in ultrapure water prepared from suitable primary standards purchased from Sigma-
180 Aldrich®.

181 **2.4.3. nanoESI-HRMS analysis**

182 Samples were analysed using a high-resolution LTQ-Orbitrap mass spectrometer (Thermo
183 Scientific™, Bremen, Germany), with a mass resolving power of 100,000 at m/z 400 and a typical
184 mass accuracy within ± 2 ppm, equipped with a chip-based nanoESI source (Triversa NanoMate
185 Advion, Ithaca, NY, USA) operating in both positive and negative ionisation mode.

186 Samples were sprayed at a gas (N_2) pressure of 0.90 psi, ionisation voltage of –1.4 kV in
187 negative ionisation mode and gas pressure of 0.30 psi, ionisation voltage of 1.8 kV in positive
188 ionisation mode, and with a transfer capillary temperature of 210 °C as used in previous studies
189 (Giorio et al., 2015, 2019a; Kourtchev et al., 2014).

190 For each sample, data were acquired in full scan in the m/z ranges 100–650 and 150–900 for 1
191 minute each in both positive and negative ionisation modes. The mass spectrometer was calibrated
192 routinely using a Pierce LTQ Velos ESI Positive Ion Calibration Solution and a Pierce ESI
193 Negative Ion Calibration Solution (Thermo Fisher).

194 The averaged spectra for each sample and each scan range were then exported as a binary list
195 of m/z values and peak intensities using the proprietary software Xcalibur™ 2.1 (Thermo
196 Scientific™, Bremen, Germany). Exported data were processed using a code written *in-house* to
197 isolate signals attributable to metal-ligand complexes of interest based on their exact mass and
198 isotopic pattern and taking into account also the possibility to form adducts with the most common
199 anions and cations present as impurities in the solvents.

200

201 **2.5. Statistical analysis**

202 Limits of detection (LODs) of both IC and ICP-MS measurements were evaluated using a
203 two-component variance regression using the ordinary least squares (OLS) regression as detailed in
204 previous studies (Badocco et al., 2015a, 2015b).

205 Data have been statistically analysed through F-test, Tukey's test, analysis of variance
206 (ANOVA), and principal component analysis (PCA) using the software Statistica 7 (StatSoft Inc.,
207 Tulsa, OK). A 95% significance level was considered for all statistical tests.
208

209 **2.6.Speciation calculations**

210 The concentration of each metal-ligand complex was calculated at the given pH value by
211 means of the software PITMAP (Di Marco, 1998). Briefly, mass balance equations are solved, i.e.
212 species concentration at equilibrium are obtained, by means of the Newton–Raphson method (Press
213 et al., 2007). The metal ions and ligands, and their concentrations were chosen on the basis of the
214 analytical results obtained in the previous sections. The input thermodynamic data (stoichiometry
215 and stability constant of the complexes, including metal-aquo-complexes) have been obtained from
216 the literature (ScQuery v.5.84, 2005). All metal ions and ligands were considered to be
217 simultaneously present in solution, in order to obtain a speciation picture which includes all
218 competitive components in solution.
219

220 **3. Results and discussion**

221 **3.1.PM_{2.5} composition**

222 Atmospheric conditions during the sampling campaign were characterised by low
223 temperatures, close to 0°C during the first part of the campaign and reaching a maximum
224 temperature of 14°C toward the end of the campaign, high relative humidity (RH), often above
225 90%, and high aerosol loading with PM_{2.5} concentrations ranging between 12 and 113 $\mu\text{g m}^{-3}$
226 (Figure 1, Table S1 and Table S2). Such conditions favour aqueous phase processing of aerosol
227 particles and fog events which create a suitable environment for coordination chemistry to occur.
228 PM_{2.5} concentrations were in the range of those observed in other northern Italian cities, such as
229 Bologna in which average PM_{2.5} values were in the range 31-59 $\mu\text{g m}^{-3}$ in the years 2011-2013
230 (Pietrogrande et al., 2014), and Milan in which average PM_{2.5} concentrations in the winter were 60
231 $\mu\text{g m}^{-3}$ in the years 2006-2009 (Perrone et al., 2012). The results of the ion chromatography analysis
232 (Figure 1, Table 1 and Table S3) show that nitrate and sulfate are the main contributing species in
233 our samples, as expected (Giorio et al., 2013, 2017).
234

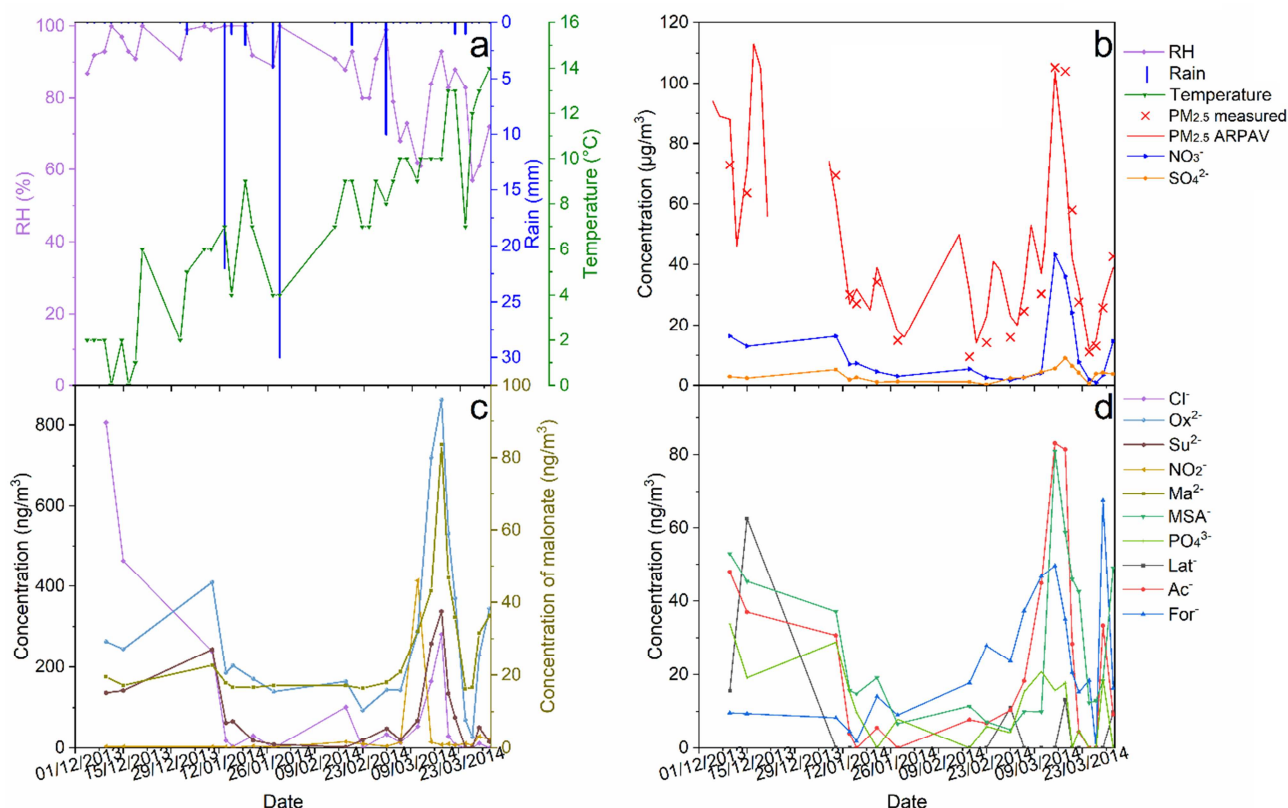
235 3.1.1. Organic acids

236 Short-chain dicarboxylic acids, i.e. oxalate, succinate, and malonate, represent abundant
237 components in our samples. These compounds have the ability to act as ligands for metal ions
238 present in $PM_{2.5}$ and therefore could affect their solubility. They can be produced by atmospheric
239 oxidation of a wide range of volatile and non-volatile organic compounds of both natural and
240 anthropic origin through gas and condensed phase reactivity (Kawamura and Bikkina, 2016; Sareen
241 et al., 2016). As expected for a continental aerosol, oxalate is the diacid present with the highest
242 concentration in our samples. The median concentrations of dicarboxylic acids (Table 1) in this
243 sampling campaign were 217 ng m^{-3} for oxalate, 19 ng m^{-3} for malonate, and 57 ng m^{-3} for
244 succinate. These values are in line with those found in Bologna, Italy, another city in the Po Valley,
245 in which average concentrations of malonate were in the range $21.7\text{-}29.7 \text{ ng m}^{-3}$ and concentrations
246 of succinate were in the range $26.8\text{-}112.1 \text{ ng m}^{-3}$ in the years 2011-2013 (Pietrogrande et al., 2014).
247 The concentration levels were not far also from those found in Hong Kong in the years 2000, where
248 average values were around 360 ng m^{-3} , 20 ng m^{-3} , and 60 ng m^{-3} for oxalate, malonate and
249 succinate, respectively (Yao et al., 2004), and 2003 when concentration values ranged between 179-
250 2372 ng m^{-3} , $38\text{-}324 \text{ ng m}^{-3}$, and $35\text{-}297 \text{ ng m}^{-3}$ for oxalate, malonate and succinate, respectively (Li
251 and Yu, 2005).

252 The ratio of malonic to succinic acid <1 for the majority of the campaign indicates a rather
253 freshly emitted organic aerosol from vehicular traffic rather than photochemically aged (Yao et al.,
254 2004). Succinate may be formed also by oxidation of unsaturated fatty acids emitted with sea spray
255 (Kerminen et al., 2000) and the presence of methanesulfonic acid (MSA) in our samples suggests
256 that atmospheric transport is taking marine biogenic emissions to our inland urban location (Yao et
257 al., 2004). Therefore, a marine contribution to succinate cannot be ruled out and the organic aerosol
258 may be more photochemically aged than predicted from the malonic to succinic acid ratio. A
259 median ratio of acetic to formic acid of about 0.5 indicates a secondary origin of carboxylic acids
260 rather than from primary emissions (Grosjean, 1992; Mkoma et al., 2012).

261 Concerning monocarboxylic acids, median concentrations in our samples were 9.8 and 17.0
262 ng m^{-3} for acetate and formate, respectively, higher than 5.4 and 0.71 ng m^{-3} found in Morogoro,
263 Tanzania (Mkoma et al., 2012). Formate concentrations were lower than those found in the US in
264 Los Angeles (49 ng m^{-3}) and Atlanta (39 ng m^{-3}) in the summer of 2010 (Liu et al., 2012). Both
265 formate and acetate concentrations were lower than those found in urban and rural $PM_{2.5}$ in Spring
266 2007 in Londrina, Brazil (Freitas et al., 2012).

267



268
269
270
271
272
273
274

Figure 1. Meteorological conditions (a), PM_{2.5} concentrations (from both the present study and the Regional Environmental Agency, ARPAV), nitrate and sulphate concentrations (b), dicarboxylic acids and nitrite concentrations (c), and other anion concentrations (d) in PM_{2.5} during the sampling campaign from the 5th December 2013 to the 1st April 2014. Lat⁻ = lactate, Ac⁻ = acetate, For⁻ = formate, MSA⁻ = methanesulfonate, Su²⁻ = succinate, Ma²⁻ = malonate, Ox²⁻ = oxalate.

Table 1. Median, maximum, 75th percentile, 25th percentile and minimum concentrations (ng m⁻³) of the inorganic and organic anions (ordered according to their retention times) determined in PM_{2.5} in the winter campaign (5th December 2013 to 1st April 2014, N=20). Lat⁻ = lactate, Ac⁻ = acetate, For⁻ = formate, MSA⁻ = methanesulfonate, Su²⁻ = succinate, Ma²⁻ = malonate, Ox²⁻ = oxalate. Measurement uncertainties are between 2-4%.

	Lat ⁻	Ac ⁻	For ⁻	MSA ⁻	Cl ⁻	NO ₂ ⁻	NO ₃ ⁻	Su ²⁻	Ma ²⁻	SO ₄ ²⁻	Ox ²⁻	PO ₄ ³⁻
Median	<LOD	9.8	17.0	17.0	23.9	7.2	6232.1	57.0	18.8	2765.9	216.9	8.8
Max	62.5	83.1	67.5	80.9	806.2	413.3	43207.3	337.7	83.6	9034.5	864.2	33.8
75th perc.	2.5	34.2	29.6	45.5	117.2	14.2	15007.0	135.1	33.0	4258.7	350.7	17.9
25th perc.	<LOD	4.3	9.3	11.1	2.8	3.01	2926.4	17.8	17.0	1727.3	143.3	<LOD
Min	<LOD	<LOD	<LOD	5.0	<LOD	<LOD	878.1	<LOD	16.3	258.7	27.7	<LOD

280

281

3.1.2. Metals

282

283

284

285

286

287

Table 2 shows the total concentration of each metal (M_T) determined in PM_{2.5}, as median of 20 samples, together with the median soluble fractions in water (M_H) and in water at a pH of 4.5 (M_A) simulating fog/rainwater. Data for each individual sample are reported in Tables S4-S9. The elements present at the highest concentrations in our samples are Na, K, Fe, Zn, Mg, Ca and Al. The soluble fractions, however, do not follow the same trend likely because the solubilisation is influenced by their speciation in the PM matrix itself, e.g. compound of origin and oxidation state

288 of the metal, and in solution. In general, the soluble fraction is larger at pH 4.5, simulating a fog or
 289 rainwater, rather than at autogenic pH (measured pH ranged between 4.5 and 5.6, median value
 290 5.0). Autogenic pH for some samples was close to, or equal to, a value of 4.5 and therefore the
 291 soluble fractions M_H and M_A were the same within uncertainty.
 292

293 **Table 2. Limits of detection (LODs), median concentrations (total amount, M_T), percentage of solubilisation at**
 294 **autogenic pH (M_H) and at an acidic pH of 4.5 (M_A) of the elements present in $PM_{2.5}$ samples collected from the**
 295 **5th December 2013 to the 1st April 2014. Measurement uncertainty is <5% (Badocco et al., 2015a).**

Element	LOD ($ng\ m^{-3}$)	M_T ($ng\ m^{-3}$)	M_H (%)	M_A (%)
Ag	0.27	<LOD		
Al	0.10	82	11	14
As	0.0070	1.2	28	40
B	0.35	570	1	1
Ba	0.083	16	0	29
Be	0.23	<LOD		
Ca	0.39	33	52	82
Cd	0.0080	0.55	26	39
Ce	0.011	0.12	4	7
Co	0.0040	0.14	7	9
Cr	0.0060	2.2	13	19
Cs	0.010	<LOD		
Cu	0.0050	11	24	35
Eu	0.0067	<LOD		
Fe	0.27	240	6	11
Ga	0.012	3	0	24
Gd	0.013	<LOD		
K	1.0	404	60	83
La	0.0030	0.06	4	6
Mg	1.1	47	11	54
Mn	0.030	7.4	29	42
Na	0.25	n.d.*	n.d.*	n.d.*
Nd	0.0040	0.027	2	1
Ni	0.16	<LOD		
P	2.8	8.9	33	59
Pb	0.0060	12	6	12
Pr	0.0010	<LOD		
Rb	0.0070	0.94	53	76
Se	0.056	0.33	41	56
Sm	0.0040	0.004	8	17
Sr	0.0030	0.58	34	55
Th	0.0075	<LOD		
Tl	0.0030	0.031	49	65
U	0.013	<LOD		
V	0.011	1.03	41	61
Zn	0.011	48	79	78

296 *n.d.=not determined, due to contaminations of blank filters

297

298 Concerning the total amounts of metals in $PM_{2.5}$, the values found in the present study were
 299 around the same order of magnitude as in other urban locations in Europe. For example, Fe median
 300 concentration was $240\ ng\ m^{-3}$ in this series of samples, which is slightly higher than $71.5\text{-}206.3$
 301 $ng\ m^{-3}$ found at five sites in the Netherlands (Mooibroek et al., 2011), within the range $54\text{-}457$

302 ng m⁻³ found in three sites in Poland (Rogula-Kozłowska et al., 2014), and within the range 0.09-
303 1152 ng m⁻³ found in rural background sites across Europe (Fomba et al., 2015). Cu median
304 concentration was 11 ng m⁻³ in this study, within the range 5-81 ng m⁻³ found across urban sites in
305 Spain (Querol et al., 2008), slightly above the range 2.5-10.9 ng m⁻³ found at five sites in the
306 Netherlands (Mooibroek et al., 2011), higher than the 2.8 ng m⁻³ in an urban site in Birmingham
307 (UK) (Pant et al., 2017) and 0.08 ng m⁻³ in Naples (Italy) (Chianese et al., 2019), within the range
308 0.10-58 ng m⁻³ found in rural background sites across Europe (Fomba et al., 2015). Zn median
309 concentration was 48 ng m⁻³ in this study, not far from the concentrations 14-420 ng m⁻³ found
310 across Spain (Querol et al., 2008), 90.5-99.5 ng m⁻³ at five sites in the Netherlands (Mooibroek et
311 al., 2011), 14.1 ng m⁻³ in an urban site in Birmingham (Pant et al., 2017), 41.3-42.4 ng m⁻³ in
312 Naples (Chianese et al., 2019) and 1.1-79.5 ng m⁻³ in rural background sites across Europe (Fomba
313 et al., 2015). Ba and Cr median concentrations were 16 and 2.2 ng m⁻³, respectively in this study.
314 These values are within the range 12-41 and 2-25 ng m⁻³ found across urban sites in Spain (Querol
315 et al., 2008) for Ba and Cr, respectively, and 4.5-11 and 2.7-3.7 ng m⁻³ found at five sites in the
316 Netherlands (Mooibroek et al., 2011) for Ba and Cr, respectively. Al median concentration of 82
317 ng m⁻³ of this study is within the range 31-457 ng m⁻³ found in three sites in Poland (Rogula-
318 Kozłowska et al., 2014). Pb, As and Cd median concentrations of 12, 1.2 and 0.55 ng m⁻³,
319 respectively, found in this study are close to the concentrations reported in the review by Csavina et
320 al. (2012) for sites affected by smelting and mining operations.

321

322 **3.2. Correlations between metals and organic ligands**

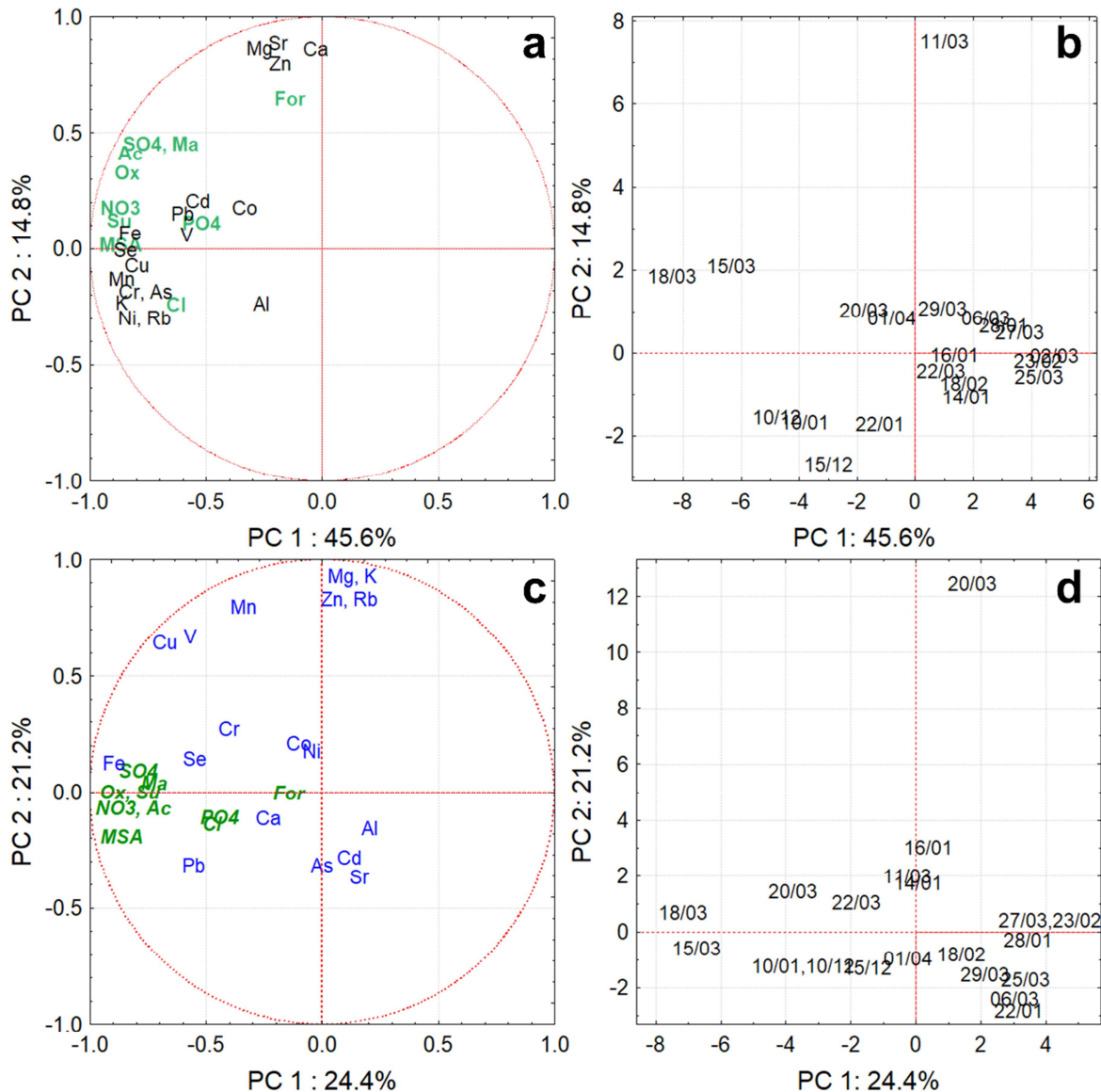
323 In order to investigate the influence of the presence of organic ligands on the solubilisation of
324 the elements a Pearson correlation test was used. Elements to be considered for this purpose were
325 selected using the ANOVA test. We selected only the elements that had a sample-to-sample
326 variance larger than the variance of the analytical measurement and a concentration value higher
327 than the LOD in at least the 70% of the samples (N = 20). Selected elements for further analysis
328 were: Al, As, B, Ba, Ca, Cd, Ce, Co, Cr, Cu, Fe, Ga, K, La, Mg, Mn, Nd, P, Pb, Rb, Se, Sm, Sr, Tl,
329 V, and Zn. An example of the results of the correlation analysis is reported in Table 3. The soluble
330 fraction of Fe (in percentage) is significantly correlated with organic species that have ligand
331 properties. The significance follows the order oxalate>succinate>malonate. A similar result was
332 obtained for Cu, while Pb is significantly correlated with oxalate. Solubility of Zn does not seem to
333 be influenced by the ligands while phosphate may influence the solubility of Pb but not that of Fe,
334 and Cu. This is further discussed in the section 3.3.

335

336
337**Table 3. p -values of the Pearson correlation tests between the soluble fraction of the elements at autogenic (M_H) and acidic (M_A) pH and selected ligands. Su^{2-} = succinate, Ma^{2-} = malonate, Ox^{2-} = oxalate.**

	Su^{2-}	Ma^{2-}	Ox^{2-}	PO_4^{3-}
Zn_H	0.66	0.58	0.50	0.47
Zn_A	0.70	0.60	0.54	0.52
Fe_H	$<10^{-4}$	$<10^{-3}$	$<10^{-6}$	0.19
Fe_A	$<10^{-4}$	$<10^{-3}$	$<10^{-5}$	0.26
Cu_H	<0.05	0.01	<0.05	0.68
Cu_A	0.03	0.04	0.01	0.64
Pb_H	<0.05	0.22	<0.01	<0.01
Pb_A	<0.05	0.49	0.05	<0.03

338

339
340
341
342
343
344
345
346**Figure 2. Loadings (a) and scores (b) of the PCA applied to the total element concentration together with all organic and inorganic anions, and loadings (c) and scores (d) of the PCA applied to the soluble fraction of the elements in water (M_H/M_T) and in water at pH 4.5 (M_A/M_T). For clarity only soluble metals in water at pH 4.5 are reported in panel c because the two fractions are always superimposed in the plane defined by the first two PCs with the exception of Cr for which the soluble fraction in water at autogenic pH is not explained by the first two PCs.**

347 Experimental data were additionally subjected to a PCA to look for possible association
348 between the elements and the organic ligands that may facilitate their solubilisation and therefore
349 enhance their bioavailability. For the PCA we considered all organic and inorganic anions listed in
350 Table 1 and Table 2, and the elements selected through the ANOVA test excluding Ba, B, La, Ce,
351 Nd, Sm, Tl and U because present at concentrations only slightly above the LOD.

352 Figure 2a and Figure 2b show the loading and score plots referred to the PCA applied to the
353 total concentration of metals. The first two principal components (PCs) explain ~60% of the
354 variance. The loading plot (Figure 2a) shows that the elements can be divided into two groups: the
355 first group correlates with PC1 and all ligands while the second group, made of Ca, Mg, Sr and Zn
356 which are characterised by a high solubility (Table 2), correlates with PC2.

357 Figure 2c and Figure 2d show the loading and score plots referred to the PCA applied to the
358 soluble fractions of the metals at autogenic pH ($M-H = M_H/M_T$) and pH 4.5 ($M-A = M_A/M_T$). The
359 first two principal components (PCs) explain only ~46% of the variance. The additional PCs did not
360 bring any information on correlations between soluble metal ions and organic ligands, so they are
361 not reported in this study.

362 The loading plot (Figure 2c) shows that the soluble fraction of Fe, both in water and at pH
363 4.5, is basically superimposed to oxalate, and the other dicarboxylic acids (succinate and malonate),
364 which is in agreement with a previous study on desert dusts (Paris and Desboeufs, 2013). PC1
365 indicates that the elements whose solubilisation is most influenced by the presence of the organic
366 ligands are Fe and Pb. Differently, the solubilisation of Cu, Mn and V are explained also by PC2.
367 Very soluble metals such as Zn, K, Rb, Mg are clustered toward the top part of the plane defined by
368 the first two PCs and strongly correlated with PC2. Sr, Ca and Al cluster together toward the
369 bottom-right of the plane defined by the first two PCs. These elements are of crustal origin and may
370 be present either in a rather refractory chemical form (Al) or be readily soluble (Ca, Sr) so that their
371 solubilisation is not much influenced by the organic component, but it may be influenced by other
372 processes (e.g. hydrolysis). Similarly, Cr-A seems to be only slightly influenced by the presence of
373 the dicarboxylic acids while Cr-H is close to the axis origin and so it is not explained by the first
374 two PCs.

375 The score plots (Figure 2b and Figure 2d) show that the samples collected on the 15th and
376 18th March 2014 are those with the highest concentrations of metals, highest soluble fraction and
377 highest concentration of organic ligands. These two days were characterised by high PM_{2.5}
378 concentrations but also high RH (Figure 1).

379

3.3. Speciation in solution

The speciation of an aqueous solution represents the qualitative and quantitative composition of the solution at the given experimental conditions. Speciation depends on temperature, pH, and concentrations of the system components. When temperature and pH are fixed, the speciation of a given metal ion M^{n+} depends on its concentration, on the concentration of all ligands in solution which can bind M^{n+} , on the concentration of all other metal ions in solution which can compete with the ligands of M^{n+} , and also on the concentration of all ligands which do not bind M^{n+} but bind the competitor metal ions. A reliable speciation model for M^{n+} can therefore be obtained only if all the solution components having binding ability are taken into account, and if stability constants of formation of the complexes are known.

A database was built, which includes the components with complexing ability detected in the soluble fractions of the PM (see Table 1 and Table 2). The inorganic and organic compounds included in the database are reported in Table 4 (first row). Monocarboxylates (acetate, formate) and methylsulfonate, although detected in the PM soluble fraction (Table 2), were not included in the database due to their low concentration in solution and especially because they are very weak complexing agents for all metal ions. Therefore, their effect on metal ion speciation can be considered negligible. Other potentially very important ligands present in the aerosol, however not determined in this study, are humic-like and fulvic-like substances. These polyfunctional macromolecules are powerful chelating agents (Borgatta and Navea, 2015; Willey et al., 2000; Win et al., 2018) but, at present, their molecular characterisation, consequent information on the stoichiometry of the complexes and their stability constants is far from complete. These substances, together with microbial proteins, may also be present as siderophores in atmospheric aqueous phases and may affect metal ion solubilisation from aerosol particles (Cheize et al., 2012; Vinatier et al., 2016). The metal ions included in the database are reported in Table 4 (first column). For the speciation calculations, each metal has been considered to be dissolved at only one oxidation state. If more oxidation states would exist for a given metal, the most stable one at environmental conditions was chosen for the speciation calculations. For example, Fe was considered to be dissolved only as Fe^{3+} , Cu only as Cu^{2+} . In the case of Fe, however, additional speciation calculations were performed considering that this metal is only in the oxidation state +2. The chosen oxidation states are explicitly stated in the first column of Table 4. Not all elements detected in the PM soluble fraction (Table 1) have been included in the database. In particular, alkaline metal ions (Na^+ , K^+ , Rb^+) have been excluded as they do not display appreciable complexing ability towards ligands in aqueous solutions. Some elements, namely V, As, and Se, are likely present as oxo-compounds in their most stable oxidation states (+5, +5 and +6, respectively), but only

414 vanadates have appreciable coordinating abilities towards ligands and were included in the
415 database. The acidity constants of the ligands (H^+ + ligand), and the stability constants of metal
416 hydroxocomplexes (metal + OH^-) were included, as H^+ and OH^- compete with the metal ions and
417 with the ligands, respectively, in the complex formation.

418 The IUPAC stability constant database was used as the source of thermodynamic data
419 regarding metal-ligand complex formation (ScQuery v.5.84, 2005). Table 4 reports the
420 stoichiometry and the stability constants of the metal-ligand complexes formed for each metal-
421 ligand pair. Many different speciation models (i.e. formation constants in different aqueous media)
422 were often reported in the literature for each given metal-ligand pair: the model chosen as the most
423 reliable (reported in Table 4) was the one obtained in aqueous solutions at the lowest level of ionic
424 strength, which better resembles atmospheric water phases such as fog and rain waters (Scheinhardt
425 et al., 2013). No mixed complexes (one metal ion + two ligands, or one ligand + two metal ions)
426 were included in the database, with the exceptions of protonated- and hydroxo-ligand complexes.

427 Speciation calculations have been performed on the basis of the thermodynamic model
428 reported in Table 4, using the metal and ligand concentration data of the sampled PM fractions. The
429 calculation was performed for all sampled solutions considering metal solubility in diluted sulfuric
430 acid solution at pH 4.5, simulating fog and rainwater. Table 5 reports the speciation data obtained
431 for the PM sampled on 10th January 2014. Data are reported as percentage of each metal species
432 relative to the total soluble amount of the same metal. Similar tables were obtained for all other
433 samples, but results do not differ significantly from those reported in Table 5 which can therefore
434 allow us to draw general conclusions.

435

436 Table 4. Inorganic/organic ligands and metal ions considered for the calculation of the speciation in PM-containing water solutions. Concerning Fe, speciation
 437 calculations were performed considering two scenarios in which Fe is present only as Fe³⁺ or only as Fe²⁺. Ox = oxalate (C₂O₄²⁻), Ma = malonate (C₃H₂O₄²⁻), Su =
 438 succinate (C₄H₄O₄²⁻). The most reliable thermodynamic model (stoichiometry and stability constants of the complexes) is reported for every metal-ligand couple as
 439 obtained from the Iupac Stability Constant database (ScQuery v.5.84, 2005). Stability constants are given as log(β) and they refer to the general reactions
 440 $m M + \ell L + h H \rightleftharpoons M_m L_\ell H_h$. Charges of the complexes are omitted for simplicity.

ligands metal ions	Cl ⁻	NO ₃ ⁻	PO ₄ ³⁻	SO ₄ ²⁻	Ox ²⁻	Ma ²⁻	Su ²⁻	OH ⁻
Al ³⁺	-	-	AlH ₂ PO ₄ 19.65 AlHPO ₄ 17.7 AlPO ₄ 13.5 AlPO ₄ OH 8.37 Al ₂ PO ₄ 17.42	AlSO ₄ 3.84 Al(SO ₄) ₂ 5.58	AlHOx 3.84 AlOx 6.97 Al(Ox) ₂ 12.93 Al(Ox) ₃ 17.88	AlMa 7.49 Al(Ma) ₂ 12.62	AlHSu 7.03 AlSu 3.63 AlSuOH -0.53 AlSu(OH) ₂ -5.55	AlOH -5.53 Al(OH) ₂ -11.3 Al(OH) ₃ -17.3 Al(OH) ₄ -23.46
Ca ²⁺	CaCl 0.42	CaNO ₃ 0.6	CaHPO ₄ 13.98	CaSO ₄ 2.19	CaOx 2.08	CaMa 2.50	CaHSu 6.18 CaSu 1.20	-
Cd ²⁺	CdCl 1.98 CdCl ₂ 2.64 CdCl ₃ 2.3	CdNO ₃ 0.40	CdHPO ₄ 15.19	CdSO ₄ 2.35	CdOx 2.52 Cd(Ox) ₂ 4.20	CdMa 2.64	CdSu 2.03	CdOH -9.80 Cd(OH) ₂ -20.19
Co ²⁺	CoCl 0.60 CoCl ₂ 0.02 CoCl ₃ -1.71 CoCl ₄ -4.51	CoNO ₃ -0.46 Co(NO ₃) ₂ -0.30	CoHPO ₄ 14.56	CoSO ₄ 2.51	CoOx 3.21 Co(Ox) ₂ 5.93	CoMa 2.92 Co(Ma) ₂ 4.60 Co(Ma) ₃ 5.30	CoSu 2.96	CoOH -8.23 Co(OH) ₂ -17.83
Cr ³⁺	CrCl -1.0	CrNO ₃ -1.91	CrPO ₄ OH 8.12 CrPO ₄ (OH) ₂ -1.92 CrPO ₄ (OH) ₃ -14.34	CrSO ₄ 1.6	CrOx 5.34 Cr(Ox) ₂ 10.51 Cr(Ox) ₃ 15.44	CrMa 7.06 Cr(Ma) ₂ 12.85 Cr(Ma) ₃ 16.15	CrSu 6.42 Cr(Su) ₂ 10.99 Cr(Su) ₃ 13.85	CrOH -4.29 Cr(OH) ₂ -9.49 Cr(OH) ₃ -18.00
Cu ²⁺	CuCl 0.83 CuCl ₂ 0.60	CuNO ₃ 0.44	CuHPO ₄ 15.67	CuSO ₄ 2.27	CuOx 4.60 Cu(Ox) ₂ 8.70	CuMa 5.13 Cu(Ma) ₂ 8.81	CuSu 3.02	CuOH -7.95 Cu(OH) ₂ -16.2 Cu(OH) ₃ -26.6
Fe ²⁺	-	-	FeH ₂ PO ₄ 22.24 FeHPO ₄ 15.94	FeSO ₄ 2.39	FeOx 2.30 Fe(Ox) ₂ 1.88	FeMa 2.24	FeSu 1.42 Fe(Su) ₂ 2.92	FeOH -9.63
Fe ³⁺	FeCl 0.67 FeCl ₂ 1.37	FeNO ₃ -0.22	FeH ₃ PO ₄ 21.48 FeH ₂ PO ₄ 23.54 FeHPO ₄ 22.34 FeH ₅ (PO ₄) ₂ 45.98 FeH ₄ (PO ₄) ₂ 46.51 FeH ₃ (PO ₄) ₂ 43.72 FeH ₇ (PO ₄) ₃ 69.12 FeH ₆ (PO ₄) ₃ 68.44	FeSO ₄ 4.27 Fe(SO ₄) ₂ 6.11	FeOx 7.53 Fe(Ox) ₂ 13.64 Fe(Ox) ₃ 18.49	FeMa 7.52 Fe(Ma) ₂ 13.29 Fe(Ma) ₃ 16.93	FeSu 7.89 Fe(Su) ₂ 13.34	FeOH -2.87 Fe(OH) ₂ -6.16 Fe(OH) ₃ -12.16 Fe(OH) ₄ -22.16
Mg ²⁺	MgCl 0.49	MgNO ₃ 0.06	MgHPO ₄ 15.04	MgSO ₄ 2.38	MgOx 2.18	MgMa 2.86	MgSu 1.47	-
Mn ²⁺	MnCl 0.85	MnNO ₃ -0.15	MnHPO ₄ 14.79	MnSO ₄ 2.26	MnOx 3.15 Mn(Ox) ₂ 4.41	MnMa 3.11	MnSu 2.26	MnOH -10.5
Ni ²⁺	NiCl -0.83	NiNO ₃ -0.22	NiHPO ₄ 14.54	NiSO ₄ 2.45	NiOx 3.46	NiMa 3.92	NiSu 3.12	NiOH -8.10

	NiCl ₂ -1.2	Ni(NO ₃) ₂ -1.0			Ni(Ox) ₂ 6.42	Ni(Ma) ₂ 6.84		Ni(OH) ₂ -16.87
Pb ²⁺	PbCl 1.50 PbCl ₂ 2.10 PbCl ₃ 2.00	PbNO ₃ 1.15	PbHPO ₄ 15.64	PbSO ₄ 2.77	PbOx 3.60 Pb(Ox) ₂ 6.10	PbMa 3.10	PbSu 2.40	PbOH -7.2 Pb(OH) ₂ -16.1 Pb(OH) ₃ -26.5
Sr ²⁺	SrCl -0.24	SrNO ₃ 0.7	SrHPO ₄ 13.72	SrSO ₄ 1.44	SrOx 1.25 Sr(Ox) ₂ 1.90	SrMa 1.30	SrSu 0.9	-
VO ₂ ⁺	VO ₂ Cl -0.38	VO ₂ NO ₃ -0.07	VO ₂ H ₂ PO ₄ 20.91 VO ₂ HPO ₄ 17.54 VO ₂ (HPO ₄) ₂ 32.88	VO ₂ SO ₄ 0.95	VO ₂ Ox 6.49 VO ₂ Ox ₂ 9.99	-	-	VO ₂ (OH) ₃ -7.1
Zn ²⁺	ZnCl 0.46	ZnNO ₃ -0.68	ZnHPO ₄ 14.86	ZnSO ₄ 2.03	ZnOx 3.42 Zn(Ox) ₂ 6.16	ZnMa 2.85	ZnSu 2.47	ZnOH -7.89 Zn(OH) ₂ -14.92
H ⁺	-	-	HPO ₄ 12.338 H ₂ PO ₄ 19.54 H ₃ PO ₄ 21.681	-	HOx 4.266 H ₂ Ox 5.54	HMa 5.70 H ₂ Ma 8.53	HSu 5.636 H ₂ Su 9.84	H ₂ O 14

441

442
443
444
445
446

Table 5. Percentages of the various metal ions species calculated on the basis of the thermodynamic model of Table 4, under the hypothesis that Fe was present as Fe(III), for the PM sampled on 10th January 2014 (concentrations in the extraction solution at pH 4.5, simulating rain droplet composition). Only species having percentages above 1% are reported. Free metal ion percentages (given as sum of percentages of Mⁿ⁺ and of its hydroxo derivatives) are reported also if below 1%.

metal ion	major species	other important species (> 5%)	minor species (< 5%)
Al ³⁺	Al(Ox) ₂ 54%	Al(Ox) ₃ 37% AlOx 8%	AlMa 1% free Al < 1%
Ca ²⁺	free Ca 91%	CaSO ₄ 8%	CaNO ₃ 1%
Cd ²⁺	free Cd 86%	CdSO ₄ 12%	CdCl 1% CdNO ₃ 1%
Co ²⁺	free Co 83%	CoSO ₄ 16%	CoOx 1%
Cr ³⁺	CrSu 25% free Cr 25%	CrMa 13% CrOx ₂ 13% CrOx 12% CrOx ₃ 9%	CrSu ₂ 1% CrMa ₂ 1%
Cu ²⁺	free Cu 68%	CuOx 21% CuSO ₄ 8%	CuOx ₂ 2% CuMa 1%
Fe ³⁺	FeOx ₂ 46%	FeOx ₃ 25% free Fe 20% FeOx 5%	FeSu 2% FeSu ₂ 1% FeHPO ₄ 1%
Mg ²⁺	free Mg 87%	MgSO ₄ 13%	
Mn ²⁺	free Mn 89%	MnSO ₄ 10%	MnOx 1%
Ni ²⁺	free Ni 84%	NiSO ₄ 14%	NiOx 2%
Pb ²⁺	free Pb 70%	PbSO ₄ 25%	PbNO ₃ 3% PbOx 2%
Sr ²⁺	free Sr 97%		SrSO ₄ 2% SrNO ₃ 1%
VO ₂ ⁺	free V 100%		
Zn ²⁺	free Zn 92%	ZnSO ₄ 6% ZnOx 2%	

447

448

449

450

451

452

453

454

455

456

457

458

459

460

461

Table 5 shows two well-defined groups of metal ions. The first group included those elements for which the main (if not only) species in solution was the free metal ion. These elements were the +2 metal cations, i.e. Ca²⁺, Cd²⁺, Co²⁺, Cu²⁺, Mg²⁺, Mn²⁺, Ni²⁺, Pb²⁺, Sr²⁺, and Zn²⁺, as well as the monocharged VO₂⁺. An example of speciation for this kind of metals is reported in Figure 3a (Zn²⁺). The only other significant species was the sulfate complex, which represented around 10% of the total metal ion in solution. For Pb²⁺ and in part also for Co²⁺ and Ni²⁺ the sulfate complex was more important, as it represented 25%, 16%, and 14%, respectively, of the total metal ion. For Cu²⁺ the oxalate complex concentration was larger than that of the sulfate complex, and the former represented 21% of total copper in solution. Copper speciation is shown in Figure 3b. These results indicated that the solubility of the first group of metal ions is scarcely affected by the presence of ligands from the aerosol. Although, the solubility contribution due to SO₄²⁻ contained in PM was generally significant, especially for the toxic Pb²⁺ ion.

The second group of elements included the +3 metal cations, i.e. Al³⁺, Cr³⁺, and Fe³⁺, for which the free metal fraction in solution was low if not negligible. The speciation for Fe³⁺ is

462 reported in Figure 3c. The main binder for these metal ions was oxalate, in particular for Al and Fe:
463 Al-oxalate complexes represented 99% of total Al in solution, and Fe-oxalate complexes accounted
464 for 76% of total Fe. Only a small fraction of Fe (~1%) was bound to phosphate. Cr displayed a
465 more complicated speciation, as oxalate was a significant but not exclusive binder. 34% of total Cr
466 was complexed by oxalate, but also Cr-succinate (26%) and Cr-malonate complexes (14%) were
467 computed to have significant concentrations in solutions. These results indicated that Al, Cr and Fe
468 solubility from aerosol was mainly, if not exclusively, determined by the ligands contained in the
469 PM among which oxalate was by far the most important. Al and Fe complexes were around 100
470 times more concentrated than the free metal ions. Therefore, Al and Fe would have dissolved less
471 (~2 orders of magnitude less) in the absence of organic aerosol components. Cr complexes were ca.
472 four times more concentrated than free Cr, so the organic aerosol components increased the
473 solubility of Cr by four times.

474 Figure 3 shows also that at higher pH, close to neutrality, condition that may be encountered in fog
475 droplets (Giulianelli et al., 2014) and biological fluids (Jayaraman et al., 2001), the speciation
476 picture changes significantly. Concerning Cu (Figure 3b), at pH close to neutrality complexation
477 becomes increasingly important, with formation of CuOx₂ and CuMa complexes. Conversely for Fe
478 (Figure 3c), complexation becomes less important and the equilibrium shifts towards formation of
479 non-soluble iron hydroxides.

480 The results obtained in this study concerning complexation of Fe³⁺ and Cu²⁺ by oxalate in simulated
481 rain droplets are consistent with those reported by Scheinhardt et al. (2013) for aerosol samples
482 from nine sites in Germany. Conversely, while Scheinhardt et al. (2013) found that nitrate was an
483 important ligand for Mn²⁺, in our study only a limited complexation of Pb²⁺ and Sr²⁺ by nitrate was
484 found. This difference may be attributed to the different conditions considered in the two studies,
485 i.e. deliquescent particles in Scheinhardt et al. (2013) vs. simulated rain droplets in the present
486 study. Our results show that ~24% of Cu is complexed by organics, in line with the results obtained
487 by Nimmo and Fones (1997) in rainwaters from two sites in northwest England. Conversely, we
488 found that only ~2% of Pb and Ni were associated with organics compared with 27-28% found by
489 Nimmo and Fones (1997) from adsorptive cathodic stripping voltammetry measurements. These
490 contrasting results may be explained by a scarce availability of ligands, already associated with
491 other metals, in our samples.

492 Availability of ligands may play a role in iron solubilisation, which was only around 6-11% on
493 average in our samples (Table 2), lower than the 44% in coal fly ash in the presence of an excess of
494 oxalic acid (Chen and Grassian, 2013) however higher than the 0.26% found in the more refractory
495 Sahelian soil (Paris and Desboeufs, 2013).

526 **Table 6. Percentages of the various metal ions species calculated on the basis of the thermodynamic model of**
 527 **Table 4, under the hypothesis that all Fe was Fe(II) rather than Fe(III), for the PM sampled on 10th January**
 528 **2014 (concentrations in the extraction solution at pH 4.5, simulating rain droplet composition). Only species**
 529 **having percentages above 1% are reported. Free metal ion percentages (given as sum of percentages of M^{nt+} and**
 530 **of its hydroxo derivatives) are reported also if below 1%. Values in blue, black and red indicate that percentages**
 531 **decreased, did not change, or increased, respectively, with respect to corresponding values of Table 5. Values in**
 532 **bold indicate that the increase/decrease was very marked.**

metal ion	major species	other important species (> 5%)	minor species (< 5%)
Al ³⁺	Al(Ox)₂ 63%	Al(Ox) ₃ 35%	AlOx 2% AlMa < 1% free Al < 1%
Ca ²⁺	free Ca 91%	CaSO ₄ 8%	CaNO ₃ 1%
Cd ²⁺	free Cd 86%	CdSO ₄ 12%	CdCl 1% CdNO ₃ 1%
Co ²⁺	free Co 81%	CoSO ₄ 16%	CoOx 3%
Cr ³⁺	CrOx₃ 47%	CrOx₂ 27% CrOx 9% CrSu 6% free Cr 6%	CrMa 4% CrSu ₂ < 1% CrMa ₂ < 1%
Cu ²⁺	free Cu 47%	CuOx 37% CuOx₂ 10% CuSO ₄ 5%	CuMa 1%
Fe ²⁺	free Fe 87%	FeSO₄ 13%	FeOx complexes < 1%
Mg ²⁺	free Mg 87%	MgSO ₄ 13%	
Mn ²⁺	free Mn 88%	MnSO ₄ 9%	MnOx 3%
Ni ²⁺	free Ni 81%	NiSO ₄ 14% NiOx 5%	
Pb ²⁺	free Pb 68%	PbSO ₄ 24% PbOx 5%	PbNO ₃ 3%
Sr ²⁺	free Sr 97%		SrSO ₄ 2% SrNO ₃ 1%
VO ₂ ⁺	free V 100%		
Zn ²⁺	free Zn 89%	ZnSO ₄ 6% ZnOx 5%	

533

534 3.4. Detection of metal-ligand complexes in urban PM_{2.5}

535 Considering the concentrations and soluble fractions of the elements (Table 2) and the
 536 complexes that are most likely to form in solution (Table 5), the metal-ligand complexes that are
 537 expected to be present at the highest concentrations in our samples are those involving the metals
 538 Fe, Cu, Mn and Pb with the ligands oxalate, malonate and succinate.

539 In order to look for signals in the mass spectra that may be attributable to these complexes, a
 540 database was built for each possible metal-ligand combination. We considered the most stable
 541 oxidation states in aqueous solution for each element: Fe(II), Fe(III), Cu(I), Cu(II), Mn(II), Mn(III),
 542 Pb(II) and Pb(IV). Concerning the ligands, we considered both the deprotonated form and the
 543 monoprotonated form for each ligand. For the metal-ligand complex formation we considered a
 544 coordination of up to 6 with the possibility to coordinate water molecules at the sites not occupied
 545 by an organic ligand. No mixed complexes (one metal ion + two ligands, or one ligand + two metal

546 ions) were included in the database. For each metal ion, 43 complexes were obtained and associated
 547 with their corresponding exact mass.

548 All possible complexes were searched for in the nanoESI-HRMS spectra as detailed in section
 549 2.4.3; results are reported in Table 7. Of all possible combination considered, five were found in the
 550 mass spectra of the samples. Among these, only one, an oxalate of iron (III) with formula
 551 $C_2H_3FeO_6$, was confirmed by analysis of standard solutions. Standard solutions of iron(III) oxalates
 552 ($[Fe^{3+}] = 2.32 \cdot 10^{-5} M$; $[Ox^{2-}] = 2.20 \cdot 10^{-4} M$) in water/methanol (50:50) at pH 2.6, 3.2 and 4.0 and in
 553 methanol at autogenic pH presented peaks in the mass spectra of the oxalate anion, and the oxalate
 554 of iron(III) with stoichiometry 2:1 (with neutral formula C_4HFeO_8). In the solution at pH 4, more
 555 similar to sample conditions, the oxalate of iron(III) with stoichiometry 1:1 (with neutral formula
 556 $C_2H_3FeO_6$) was also detected, thus confirming the signal that was assigned in the real samples
 557 (species in bold in Table 7). However, the ratio between C_4HFeO_8 and $C_2H_3FeO_6$ is about 10:1 in
 558 the standard solution while $C_2H_3FeO_6$ is the only detected species in the real samples. This
 559 discrepancy between real samples and standard solutions may be due to different oxalate
 560 concentrations in the real samples and/or matrix effects that might have influenced fragmentation in
 561 the ESI source. Further work is needed to confirm the presence of metal-ligand complexes in
 562 atmospheric aerosol, including measurements without prior extraction in an aqueous or organic
 563 solvent that may introduce artefacts.

564

565 **Table 7. Detected metal-ligand (ML) complexes in nanoESI-HRMS spectra (in negative ionisation mode) of**
 566 **PM_{2.5} samples collected from the 5th December 2013 to the 1st April 2014. The species in bold was confirmed by**
 567 **analysis of standard solutions.**

Formula	Metal ion	Ligands	Coordinating water molecules	Adducts	Detected ion	Samples in which ML were detected
$C_8H_{16}FeO_{11}$	Fe^{2+}	2 x ($Su^{2-} + H^+$)	3 x (H_2O)	Cl^- , For^-	$[ML+Cl+For]^{2-}$	QF11-W
$C_2H_3FeO_6$	Fe^{3+}	Ox^{2-}	$H_2O + OH^-$	Cl^-	$[ML+Cl]^-$	QF8-W, QF9-W
$C_{16}H_{23}MnO_{17}$	Mn^{3+}	4 x ($Su^{2-} + H^+$)	H_2O	For^- , Ac^-	$[ML+For+Ac]^{3-}$	QF6-W, QF16-W
$C_6H_7CuO_9Na$	Cu^{2+}	2 x Ma^{2-}	H_2O	Na^+	$[ML+Na]^-$	QF1-W, QF9-W, QF10-W
$C_{16}H_{27}CuO_{17}N$	Cu^{2+}	4 x ($Su^{2-} + H^+$)	H_2O	NH_4^+ , For^-	$[ML+NH_4+For]^-$	QF15-W, QF17-W, QF18-W

568

569 The samples in which the iron oxalate complex was detected were collected on the 3rd January
 570 2014 and on the 8th January 2014. These two days were characterised by a relatively high aerosol
 571 concentration (PM_{2.5} 74 $\mu g m^{-3}$ on the 8th January) and ambient temperature was close to the
 572 dewpoint temperature (Lawrence, 2005) therefore indicating a high probability of fog formation
 573 favouring aqueous phase chemistry. These were the only two days in which both conditions (high
 574 aerosol loading and high probability of fog formation) occurred simultaneously.

575

576 4. Conclusions

577 We investigated the formation of metal-ligand complexes, and how this process may affect
578 the solubility of metals, in urban atmospheric aerosol samples collected in the city centre of Padua
579 (Italy) from the 5th December 2013 to the 1st April 2014. Short-chain dicarboxylic acids, i.e.
580 oxalate, succinate, and malonate, were abundant aerosol components in the collected samples that
581 possess ligand properties. We found that organic ligand concentrations are significantly correlated
582 with the soluble fraction of non-readily soluble metals, such as Fe.

583 PCA applied to the soluble fractions of all metals and the concentration of both organic and
584 inorganic anions showed that very soluble metals, such as Zn, K, Rb, and Mg, are not associated
585 with the presence of the organic ligands. Fe and Pb, on the contrary, are the elements whose
586 solubility is strongly associated with the presence of the organic ligands. A speciation analysis in
587 solution at pH 4.5, simulating fog/rainwater, pointed out that many metals are either partly
588 complexed with oxalate, malonate and succinate, like Cu, Zn, Mn, Pb, and Ni, or completely
589 complexed with the same diacids, like Al, Cr and Fe. The solubility increments of Al and Fe due to
590 aerosol components can be estimated to be around two orders of magnitudes, while for Cr the
591 solubility is increased by four times due to the presence of diacids. According to our results, the
592 oxidation state of Fe can have a significant effect on the speciation of this and of other metal ions
593 dissolving in aqueous solution. Further studies appear necessary to obtain information on the
594 oxidation state of Fe, both when contained in PM and once released in an aqueous solution, to allow
595 an accurate prediction of the speciation picture of PM components.

596 Direct analysis of aerosol extracts in methanol with nanoESI-HRMS showed the presence of a
597 signal of a 1:1 complex between Fe(III) and oxalate in two samples collected on days characterised
598 by high aerosol loading and high probability of fog formation, indicating that these complexes can
599 be identified directly.

600 The study here reported considers metal speciation at equilibrium and confirms, using both
601 quantitative data and a thermodynamic model, that important environmental and health properties
602 of the aerosol may be influenced by metal-ligand interactions in the specific media. The solubility
603 changes of metal ions potentially induced by complexation with organics affects the bioaccessibility
604 (Wiseman, 2015) of the metals themselves. Formation of complexes can also impact redox
605 chemistry, therefore the ability of metals to deplete antioxidants in the lungs once particles are
606 inhaled and come into contact with lung fluids. Further work is needed to investigate the kinetic of
607 solubilisation of the metals and how it is affected by other aerosol components.

608

609 **Acknowledgements**

610 This work was partly funded by the Supporting TAlent in ReSearch@University of Padova
611 STARS-StG MOCAA to CG and by the European Research Council ERC consolidator grant
612 279405 to MK.

613

614 **References**

615 Badocco, D., Lavagnini, I., Mondin, A. and Pastore, P.: Estimation of the uncertainty of the
616 quantification limit, *Spectrochim. Acta - Part B At. Spectrosc.*, 96, 8–11,
617 doi:10.1016/j.sab.2014.03.013, 2014.

618 Badocco, D., Lavagnini, I., Mondin, A. and Pastore, P.: Effect of multiple error sources on the
619 calibration uncertainty, *Food Chem.*, 177, 147–151, doi:10.1016/j.foodchem.2015.01.020, 2015a.

620 Badocco, D., Lavagnini, I., Mondin, A., Tapparo, A. and Pastore, P.: Limit of detection in the
621 presence of instrumental and non-instrumental errors : study of the possible sources of error and
622 application to the analysis of 41 elements at trace levels by inductively coupled plasma-mass
623 spectrometry technique, *Spectrochim. Acta Part B At. Spectrosc.*, 107, 178–184,
624 doi:10.1016/j.sab.2015.03.009, 2015b.

625 Beiderwieden, E., Wrzesinsky, T. and Klemm, O.: Chemical characterization of fog and rain
626 water collected at the eastern Andes cordillera, *Hydrol. Earth Syst. Sci. Discuss.*, 2(3), 863–885,
627 doi:10.5194/hessd-2-863-2005, 2005.

628 Birmili, W., Allen, A. G., Bary, F. and Harrison, R. M.: Trace Metal Concentrations and
629 Water Solubility in Size-Fractionated Atmospheric Particles and Influence of Road Traffic,
630 *Environ. Sci. Technol.*, 40(4), 1144–1153, doi:10.1021/es0486925, 2006.

631 Borgatta, J. and Navea, J. G.: Fate of aqueous iron leached from tropospheric aerosols during
632 atmospheric acidic processing: A study of the effect of humic-like substances, *WIT Trans. Ecol.*
633 *Environ.*, 198(Iii), 155–166, doi:10.2495/AIR150131, 2015.

634 Burnett, R., Chen, H., Szyszkowicz, M., Fann, N., Hubbell, B., Pope, C. A., Apte, J. S.,
635 Brauer, M., Cohen, A., Weichenthal, S., Coggins, J., Di, Q., Brunekreef, B., Frostad, J., Lim, S. S.,
636 Kan, H., Walker, K. D., Thurston, G. D., Hayes, R. B., Lim, C. C., Turner, M. C., Jerrett, M.,
637 Krewski, D., Gapstur, S. M., Diver, W. R., Ostro, B., Goldberg, D., Crouse, D. L., Martin, R. V.,
638 Peters, P., Pinault, L., Tjepkema, M., van Donkelaar, A., Villeneuve, P. J., Miller, A. B., Yin, P.,
639 Zhou, M., Wang, L., Janssen, N. A. H., Marra, M., Atkinson, R. W., Tsang, H., Quoc Thach, T.,
640 Cannon, J. B., Allen, R. T., Hart, J. E., Laden, F., Cesaroni, G., Forastiere, F., Weinmayr, G.,
641 Jaensch, A., Nagel, G., Concin, H. and Spadaro, J. V.: Global estimates of mortality associated with

- 642 long-term exposure to outdoor fine particulate matter, *Proc. Natl. Acad. Sci.*, 115(38), 9592–9597,
643 doi:10.1073/pnas.1803222115, 2018.
- 644 Cheize, M., Sarthou, G., Croot, P. L., Bucciarelli, E., Baudoux, A. C. and Baker, A. R.: Iron
645 organic speciation determination in rainwater using cathodic stripping voltammetry, *Anal. Chim.*
646 *Acta*, 736, 45–54, doi:10.1016/j.aca.2012.05.011, 2012.
- 647 Chen, H. and Grassian, V. H.: Iron dissolution of dust source materials during simulated
648 acidic processing: The effect of sulfuric, acetic, and oxalic acids, *Environ. Sci. Technol.*, 47(18),
649 10312–10321, doi:10.1021/es401285s, 2013.
- 650 Chen, L. C. and Lippmann, M.: Effects of Metals within Ambient Air Particulate Matter (PM)
651 on Human Health, *Inhal. Toxicol.* [online] Available from:
652 <http://www.tandfonline.com/doi/abs/10.1080/08958370802105405?journalCode=iiht20> (Accessed
653 19 November 2015), 2009.
- 654 Chianese, E., Tirimberio, G. and Riccio, A.: PM_{2.5} and PM₁₀ in the urban area of Naples:
655 chemical composition, chemical properties and influence of air masses origin, *J. Atmos. Chem.*,
656 76(2), 151–169, doi:10.1007/s10874-019-09392-3, 2019.
- 657 Cotton, F. A. and Wilkinson, G.: *Advanced Inorganic Chemistry*, Fifth Edit., John Wiley and
658 Sons, Inc., 1988.
- 659 Csavina, J., Field, J., Taylor, M. P., Gao, S., Landázuri, A., Betterton, E. A. and Sáez, A. E.:
660 A review on the importance of metals and metalloids in atmospheric dust and aerosol from mining
661 operations, *Sci. Total Environ.*, 433, 58–73, doi:10.1016/j.scitotenv.2012.06.013, 2012.
- 662 Decesari, S., Sowlat, M. H., Hasheminassab, S., Sandrini, S., Gilardoni, S., Facchini, M. C.,
663 Fuzzi, S. and Sioutas, C.: Enhanced toxicity of aerosol in fog conditions in the Po Valley, Italy,
664 *Atmos. Chem. Phys. Discuss.*, (February), 1–19, doi:10.5194/acp-2017-118, 2017.
- 665 Deguillaume, L., Leriche, M., Desboeufs, K., Mailhot, G., George, C. and Chaumerliac, N.:
666 Transition metals in atmospheric liquid phases: Sources, reactivity, and sensitive parameters, *Chem.*
667 *Rev.*, 105, 3388–3431, doi:10.1021/cr040649c, 2005.
- 668 DePalma, S. G. S., Arnold, W. R., McGeer, J. C., Dixon, D. G. and Smith, D. S.: Effects of
669 dissolved organic matter and reduced sulphur on copper bioavailability in coastal marine
670 environments., *Ecotoxicol. Environ. Saf.*, 74(3), 230–7, doi:10.1016/j.ecoenv.2010.12.003, 2011.
- 671 Elzinga, E. J., Gao, Y., Fitts, J. P. and Tappero, R.: Iron speciation in urban dust, *Atmos.*
672 *Environ.*, 45(26), 4528–4532, doi:10.1016/j.atmosenv.2011.05.042, 2011.
- 673 Fomba, K. W., Van Pinxteren, D., Müller, K., Iinuma, Y., Lee, T., Collett, J. L. and
674 Herrmann, H.: Trace metal characterization of aerosol particles and cloud water during HCCT
675 2010, *Atmos. Chem. Phys.*, 15(15), 8751–8765, doi:10.5194/acp-15-8751-2015, 2015.

- 676 Franzetti, A., Gandolfi, I., Gaspari, E., Ambrosini, R. and Bestetti, G.: Seasonal variability of
677 bacteria in fine and coarse urban air particulate matter, *Appl. Microbiol. Biotechnol.*, 90(2), 745–
678 753, doi:10.1007/s00253-010-3048-7, 2011.
- 679 Freitas, A. de M., Martins, L. D. and Solci, M. C.: Size-segregated particulate matter and
680 carboxylic acids over urban and rural sites in Londrina City, Brazil, *J. Braz. Chem. Soc.*, 23(5),
681 921–930, doi:10.1590/S0103-50532012000500018, 2012.
- 682 Giorio, C., Tapparo, A., Scapellato, M. L., Carrieri, M., Apostoli, P. and Bartolucci, G. B.:
683 Field comparison of a personal cascade impactor sampler, an optical particle counter and CEN-EU
684 standard methods for PM₁₀, PM_{2.5} and PM₁ measurement in urban environment, *J. Aerosol Sci.*,
685 65, 111–120, doi:10.1016/j.jaerosci.2013.07.013, 2013.
- 686 Giorio, C., Moyroud, E., Glover, B. J., Skelton, P. C. and Kalberer, M.: Direct Surface
687 Analysis Coupled to High-Resolution Mass Spectrometry Reveals Heterogeneous Composition of
688 the Cuticle of *Hibiscus trionum* Petals, *Anal. Chem.*, 87(19), 9900–9907,
689 doi:10.1021/acs.analchem.5b02498, 2015.
- 690 Giorio, C., Marton, D., Formenton, G. and Tapparo, A.: Formation of Metal–Cyanide
691 Complexes in Deliquescent Airborne Particles: A New Possible Sink for HCN in Urban
692 Environments, *Environ. Sci. Technol.*, 51(24), 14107–14113, doi:10.1021/acs.est.7b03123, 2017.
- 693 Giorio, C., Bortolini, C., Kourtchev, I., Tapparo, A., Bogialli, S. and Kalberer, M.: Direct
694 target and non-target analysis of urban aerosol sample extracts using atmospheric pressure
695 photoionisation high-resolution mass spectrometry, *Chemosphere*, 224, 786–795,
696 doi:10.1016/j.chemosphere.2019.02.151, 2019a.
- 697 Giorio, C., Pizzini, S., Marchiori, E., Piazza, R., Grigolato, S., Zanetti, M., Cavalli, R.,
698 Simoncin, M., Soldà, L., Badocco, D. and Tapparo, A.: Sustainability of using vineyard pruning
699 residues as an energy source: Combustion performances and environmental impact, *Fuel*, 243, 371–
700 380, doi:10.1016/j.fuel.2019.01.128, 2019b.
- 701 Giulianelli, L., Gilardoni, S., Tarozzi, L., Rinaldi, M., Decesari, S., Carbone, C., Facchini, M.
702 C. and Fuzzi, S.: Fog occurrence and chemical composition in the Po valley over the last twenty
703 years, *Atmos. Environ.*, 98, 394–401, doi:10.1016/j.atmosenv.2014.08.080, 2014.
- 704 Grosjean, D.: Formic acid and acetic acid: Emissions, atmospheric formation and dry
705 deposition at two southern California locations, *Atmos. Environ. Part A, Gen. Top.*, 26(18), 3279–
706 3286, doi:10.1016/0960-1686(92)90343-J, 1992.
- 707 Harrison, R. M., Giorio, C., Beddows, D. C. S. and Dall’Osto, M.: Size distribution of
708 airborne particles controls outcome of epidemiological studies, *Sci. Total Environ.*, 409(2), 289–
709 293, doi:10.1016/j.scitotenv.2010.09.043, 2010.

- 710 Jayaraman, S., Song, Y., Vetrivel, L., Shankar, L. and Verkman, A. S.: Noninvasive in vivo
711 fluorescence measurement of airway-surface liquid depth, salt concentration, and pH, *J. Clin.*
712 *Invest.*, 107(3), 317–324, doi:10.1172/JCI11154, 2001.
- 713 Jickells, T. D., An, Z. S., Andersen, K. K., Baker, A. R., Bergametti, G., Brooks, N., Cao, J.
714 J., Boyd, P. W., Duce, R. A., Hunter, K. A., Kawahata, H., Kubilay, N., laRoche, J., Liss, P. S.,
715 Mahowald, N., Prospero, J. M., Ridgwell, A. J., Tegen, I. and Torres, R.: Global iron connections
716 between desert dust, ocean biogeochemistry, and climate., *Science*, 308(5718), 67–71,
717 doi:10.1126/science.1105959, 2005.
- 718 Kawamura, K. and Bikkina, S.: A review of dicarboxylic acids and related compounds in
719 atmospheric aerosols: Molecular distributions, sources and transformation, *Atmos. Res.*, 170, 140–
720 160, doi:10.1016/j.atmosres.2015.11.018, 2016.
- 721 Kerminen, V.-M., Ojanen, C., Pakkanen, T., Hillamo, R., Aurela, M. and Meriläinen, J.:
722 LOW-MOLECULAR-WEIGHT DICARBOXYLIC ACIDS IN AN URBAN AND RURAL
723 ATMOSPHERE, *J. Aerosol Sci.*, 31(3), 349–362, doi:10.1016/S0021-8502(99)00063-4, 2000.
- 724 Kourtchev, I., O'Connor, I. P., Giorio, C., Fuller, S. J., Kristensen, K., Maenhaut, W.,
725 Wenger, J. C., Sodeau, J. R., Glasius, M. and Kalberer, M.: Effects of anthropogenic emissions on
726 the molecular composition of urban organic aerosols: An ultrahigh resolution mass spectrometry
727 study, *Atmos. Environ.*, 89, 525–532, doi:10.1016/j.atmosenv.2014.02.051, 2014.
- 728 Lawrence, M. G.: The relationship between relative humidity and the dewpoint temperature in
729 moist air: A simple conversion and applications, *Bull. Am. Meteorol. Soc.*, 86(2), 225–233,
730 doi:10.1175/BAMS-86-2-225, 2005.
- 731 Lelieveld, J., Evans, J. S., Fnais, M., Giannadaki, D. and Pozzer, A.: The contribution of
732 outdoor air pollution sources to premature mortality on a global scale, *Nature*, 525(7569), 367–371,
733 doi:10.1038/nature15371, 2015.
- 734 Lelieveld, J., Klingmüller, K., Pozzer, A., Pöschl, U., Fnais, M., Daiber, A. and Münzel, T.:
735 Cardiovascular disease burden from ambient air pollution in Europe reassessed using novel hazard
736 ratio functions, *Eur. Heart J.*, 1–7, doi:10.1093/eurheartj/ehz135, 2019.
- 737 Li, Y. C. and Yu, J. Z.: Simultaneous determination of mono- and dicarboxylic acids, ω -oxo-
738 carboxylic acids, midchain ketocarboxylic acids, and aldehydes in atmospheric aerosol samples,
739 *Environ. Sci. Technol.*, 39(19), 7616–7624, doi:10.1021/es050896d, 2005.
- 740 Liu, J., Zhang, X., Parker, E. T., Veres, P. R., Roberts, J. M., de Gouw, J. A., Hayes, P. L.,
741 Jimenez, J. L., Murphy, J. G., Ellis, R. A., Huey, L. G. and Weber, R. J.: On the gas-particle
742 partitioning of soluble organic aerosol in two urban atmospheres with contrasting emissions: 2. Gas
743 and particle phase formic acid, *J. Geophys. Res. Atmos.*, 117(D21), n/a-n/a,

744 doi:10.1029/2012JD017912, 2012.

745 Majestic, B. J., Schauer, J. J., Shafer, M. M., Turner, J. R., Fine, P. M., Singh, M. and Sioutas,
746 C.: Development of a Wet-Chemical Method for the Speciation of Iron in Atmospheric Aerosols,
747 Environ. Sci. Technol., 40(7), 2346–2351, doi:10.1021/es052023p, 2006.

748 Di Marco, V. B.: Studio della formazione di complessi tra alluminio e molecole di interesse
749 ambientale, biologico e farmaceutico, 11 November. [online] Available from:
750 <http://paduaresearch.cab.unipd.it/7349/> (Accessed 25 May 2019), 1998.

751 Mkoma, S. L., da Rocha, G. O., da Silva, J. D. S. and de Andrade, J. B.: Characteristics of
752 Low-Molecular Weight Carboxylic Acids in PM_{2.5} and PM₁₀ Ambient Aerosols From Tanzania,
753 in Atmospheric Aerosols - Regional Characteristics - Chemistry and Physics, pp. 203–219, InTech.,
754 2012.

755 Mooibroek, D., Schaap, M., Weijers, E. P. and Hoogerbrugge, R.: Source apportionment and
756 spatial variability of PM_{2.5} using measurements at five sites in the Netherlands, Atmos. Environ.,
757 45(25), 4180–4191, doi:10.1016/j.atmosenv.2011.05.017, 2011.

758 Nieberding, F., Breuer, B., Braeckevelt, E., Klemm, O., Song, Q. and Zhang, Y.: Fog water
759 chemical composition on ailaoshan mountain, Yunnan province, SW China, Aerosol Air Qual. Res.,
760 18(1), 37–48, doi:10.4209/aaqr.2017.01.0060, 2018.

761 Nimmo, M. and Fones, G. R.: The potential pool of Co, Ni, Cu, Pb and Cd organic
762 complexing ligands in coastal and urban rain waters, Atmos. Environ., 31(5), 693–702,
763 doi:10.1016/S1352-2310(96)00243-9, 1997.

764 Oberdörster, G., Oberdörster, E. and Oberdörster, J.: Nanotoxicology: An emerging discipline
765 evolving from studies of ultrafine particles, Environ. Health Perspect., 113(7), 823–839,
766 doi:10.1289/ehp.7339, 2005.

767 Okochi, H. and Brimblecombe, P.: Potential trace metal-organic complexation in the
768 atmosphere., ScientificWorldJournal., 2, 767–86, doi:10.1100/tsw.2002.132, 2002.

769 Pant, P., Shi, Z., Pope, F. D. and Harrison, R. M.: Characterization of traffic-related
770 particulate matter emissions in a road tunnel in Birmingham, UK: Trace metals and organic
771 molecular markers, Aerosol Air Qual. Res., 17(1), 117–130, doi:10.4209/aaqr.2016.01.0040, 2017.

772 Paris, R. and Desboeufs, K. V.: Effect of atmospheric organic complexation on iron-bearing
773 dust solubility, Atmos. Chem. Phys., 13(9), 4895–4905, doi:10.5194/acp-13-4895-2013, 2013.

774 Paris, R., Desboeufs, K. V. and Journet, E.: Variability of dust iron solubility in atmospheric
775 waters: Investigation of the role of oxalate organic complexation, Atmos. Environ., 45(36), 6510–
776 6517, doi:10.1016/j.atmosenv.2011.08.068, 2011.

777 Perrone, M. G., Gualtieri, M., Ferrero, L., Porto, C. Lo, Udisti, R., Bolzacchini, E. and

- 778 Camatini, M.: Seasonal variations in chemical composition and in vitro biological effects of fine
779 PM from Milan, *Chemosphere*, doi:10.1016/j.chemosphere.2009.12.071, 2010.
- 780 Perrone, M. G., Larsen, B. R., Ferrero, L., Sangiorgi, G., De Gennaro, G., Udisti, R.,
781 Zangrando, R., Gambaro, A. and Bolzacchini, E.: Sources of high PM_{2.5} concentrations in Milan,
782 Northern Italy: Molecular marker data and CMB modelling, *Sci. Total Environ.*, 414, 343–355,
783 doi:10.1016/j.scitotenv.2011.11.026, 2012.
- 784 Pietrogrande, M. C., Bacco, D., Visentin, M., Ferrari, S. and Poluzzi, V.: Polar organic
785 marker compounds in atmospheric aerosol in the Po Valley during the Supersito campaigns — Part
786 1: Low molecular weight carboxylic acids in cold seasons, *Atmos. Environ.*, 86, 164–175,
787 doi:10.1016/j.atmosenv.2013.12.022, 2014.
- 788 Press, W. H., Teukolsky, S. A., Vetterling, W. T., Flannery, B. P. and Cambridge University
789 Press: *Numerical recipes: the art of scientific computing*. [online] Available from:
790 [https://www.cambridge.org/it/academic/subjects/mathematics/numerical-recipes/numerical-recipes-](https://www.cambridge.org/it/academic/subjects/mathematics/numerical-recipes/numerical-recipes-art-scientific-computing-3rd-edition?format=HB&utm_source=shortlink&utm_medium=shortlink&utm_campaign=numericalrecipes)
791 [art-scientific-computing-3rd-](https://www.cambridge.org/it/academic/subjects/mathematics/numerical-recipes/numerical-recipes-art-scientific-computing-3rd-edition?format=HB&utm_source=shortlink&utm_medium=shortlink&utm_campaign=numericalrecipes)
792 [edition?format=HB&utm_source=shortlink&utm_medium=shortlink&utm_campaign=numericalrec-](https://www.cambridge.org/it/academic/subjects/mathematics/numerical-recipes/numerical-recipes-art-scientific-computing-3rd-edition?format=HB&utm_source=shortlink&utm_medium=shortlink&utm_campaign=numericalrecipes)
793 [ipes](https://www.cambridge.org/it/academic/subjects/mathematics/numerical-recipes/numerical-recipes-art-scientific-computing-3rd-edition?format=HB&utm_source=shortlink&utm_medium=shortlink&utm_campaign=numericalrecipes) (Accessed 25 May 2019), 2007.
- 794 Querol, X., Alastuey, A., Moreno, T., Viana, M. M., Castillo, S., Pey, J., Rodríguez, S.,
795 Artiñano, B., Salvador, P., Sánchez, M., Garcia Dos Santos, S., Herce Garraleta, M. D., Fernandez-
796 Patier, R., Moreno-Grau, S., Negral, L., Minguillón, M. C., Monfort, E., Sanz, M. J., Palomo-
797 Marín, R., Pinilla-Gil, E., Cuevas, E., de la Rosa, J. and Sánchez de la Campa, A.: Spatial and
798 temporal variations in airborne particulate matter (PM₁₀ and PM_{2.5}) across Spain 1999–2005,
799 *Atmos. Environ.*, 42(17), 3964–3979, doi:10.1016/j.atmosenv.2006.10.071, 2008.
- 800 Raaschou-Nielsen, O., Andersen, Z. J., Beelen, R., Samoli, E., Stafoggia, M., Weinmayr, G.,
801 Hoffmann, B., Fischer, P., Nieuwenhuijsen, M. J., Brunekreef, B., Xun, W. W., Katsouyanni, K.,
802 Dimakopoulou, K., Sommar, J., Forsberg, B., Modig, L., Oudin, A., Oftedal, B., Schwarze, P. E.,
803 Nafstad, P., De Faire, U., Pedersen, N. L., Östenson, C.-G., Fratiglioni, L., Penell, J., Korek, M.,
804 Pershagen, G., Eriksen, K. T., Sørensen, M., Tjønneland, A., Ellermann, T., Eeftens, M., Peeters, P.
805 H., Meliefste, K., Wang, M., Bueno-de-Mesquita, B., Key, T. J., de Hoogh, K., Concin, H., Nagel,
806 G., Vilier, A., Gioni, S., Krogh, V., Tsai, M.-Y., Ricceri, F., Sacerdote, C., Galassi, C., Migliore,
807 E., Ranzi, A., Cesaroni, G., Badaloni, C., Forastiere, F., Tamayo, I., Amiano, P., Dorronsoro, M.,
808 Trichopoulou, A., Bamia, C., Vineis, P. and Hoek, G.: Air pollution and lung cancer incidence in 17
809 European cohorts: prospective analyses from the European Study of Cohorts for Air Pollution
810 Effects (ESCAPE), *Lancet Oncol.*, 14(9), 813–822, doi:10.1016/S1470-2045(13)70279-1, 2013.
- 811 Rodhe, H., Dentener, F. and Schulz, M.: The Global Distribution of Acidifying Wet

- 812 Deposition, *Environ. Sci. Technol.*, 36(20), 4382–4388, doi:10.1021/es020057g, 2002.
- 813 Rogula-Kozłowska, W., Klejnowski, K., Rogula-Kopiec, P., Ośródk, L., Krajny, E.,
814 Błaszczak, B. and Mathews, B.: Spatial and seasonal variability of the mass concentration and
815 chemical composition of PM 2.5 in Poland, *Air Qual. Atmos. Heal.*, 7(1), 41–58,
816 doi:10.1007/s11869-013-0222-y, 2014.
- 817 Sareen, N., Carlton, A. G., Surratt, J. D., Gold, A., Lee, B., Lopez-Hilfiker, F. D., Mohr, C.,
818 Thornton, J. A., Zhang, Z., Lim, Y. B. and Turpin, B. J.: Identifying precursors and aqueous organic
819 aerosol formation pathways during the SOAS campaign, *Atmos. Chem. Phys.*, 16(22), 14409–
820 14420, doi:10.5194/acp-16-14409-2016, 2016.
- 821 Scheinhardt, S., Müller, K., Spindler, G. and Herrmann, H.: Complexation of trace metals in
822 size-segregated aerosol particles at nine sites in Germany, *Atmos. Environ.*, 74, 102–109,
823 doi:10.1016/j.atmosenv.2013.03.023, 2013.
- 824 Schroth, A. W., Crusius, J., Sholkovitz, E. R. and Bostick, B. C.: Iron solubility driven by
825 speciation in dust sources to the ocean, *Nat. Geosci.*, 2(5), 337–340, doi:10.1038/ngeo501, 2009.
- 826 ScQuery v.5.84: The Iupac Stability Constant Database, Academic Software, Copyright,
827 2005.
- 828 Shiraiwa, M., Ueda, K., Pozzer, A., Lammel, G., Kampf, C. J., Fushimi, A., Enami, S.,
829 Arangio, A. M., Fröhlich-Nowoisky, J., Fujitani, Y., Furuyama, A., Lakey, P. S. J., Lelieveld, J.,
830 Lucas, K., Morino, Y., Pöschl, U., Takahama, S., Takami, A., Tong, H., Weber, B., Yoshino, A.
831 and Sato, K.: Aerosol Health Effects from Molecular to Global Scales, *Environ. Sci. Technol.*,
832 51(23), 13545–13567, doi:10.1021/acs.est.7b04417, 2017.
- 833 Tong, H.-J., Fitzgerald, C., Gallimore, P. J., Kalberer, M., Kuimova, M. K., Seville, P. C.,
834 Ward, A. D. and Pope, F. D.: Rapid interrogation of the physical and chemical characteristics of
835 salbutamol sulphate aerosol from a pressurised metered-dose inhaler (pMDI), *Chem. Commun.*
836 (Camb), 50(3), 3–6, doi:10.1039/c4cc05803h, 2014.
- 837 Topinka, J., Rossner, P., Milcova, A., Schmuczerova, J., Svecova, V. and Sram, R. J.: DNA
838 adducts and oxidative DNA damage induced by organic extracts from PM2.5 in an acellular assay,
839 *Toxicol. Lett.*, 202(3), 186–192, doi:10.1016/J.TOXLET.2011.02.005, 2011.
- 840 Vinatier, V., Wirgot, N., Joly, M., Sancelme, M., Abrantes, M., Deguillaume, L. and Delort,
841 A. M.: Siderophores in cloud waters and potential impact on atmospheric chemistry: Production by
842 microorganisms isolated at the puy de Dôme station, *Environ. Sci. Technol.*, 50(17), 9315–9323,
843 doi:10.1021/acs.est.6b02335, 2016.
- 844 Walna, B.: Results of long-term observations of basic physico-chemical data of atmospheric
845 precipitation in a protected area in Western Poland, *Atmos. Pollut. Res.*, 6(4), 651–661,

846 doi:10.5094/apr.2015.074, 2015.

847 Wang, P., Bi, S. P., Zhou, Y. P., Tao, Q. S., Gan, W. X., Xu, Y., Hong, Z. and Cai, W. S.:
848 Study of aluminium distribution and speciation in atmospheric particles of different diameters in
849 Nanjing, China, *Atmos. Environ.*, 41(27), 5788–5796, doi:10.1016/j.atmosenv.2007.01.064, 2007.

850 Wang, Y., Yu, W., Pan, Y. and Wu, D.: Acid neutralization of precipitation in Northern
851 China, *J. Air Waste Manag. Assoc.*, 62(2), 204–211, doi:10.1080/10473289.2011.640761, 2012.

852 Wei, J., Yu, H., Wang, Y. and Verma, V.: Complexation of Iron and Copper in Ambient
853 Particulate Matter and Its Effect on the Oxidative Potential Measured in a Surrogate Lung Fluid,
854 *Environ. Sci. Technol.*, 53(3), 1661–1671, doi:10.1021/acs.est.8b05731, 2019.

855 WHO, W. H. O.: Ambient Air Pollution: A global assessment of exposure and burden of
856 disease, *World Heal. Organ.*, doi:9789241511353, 2016.

857 Willey, J. D., Kieber, R. J., Williams, K. H., Crozier, J. S., Skrabal, S. A. and Avery, G. B.:
858 Temporal variability of iron speciation in coastal rainwater, *J. Atmos. Chem.*, 37(2), 185–205,
859 doi:10.1023/A:1006421624865, 2000.

860 Win, M. S., Tian, Z., Zhao, H., Xiao, K., Peng, J., Shang, Y., Wu, M., Xiu, G., Lu, S.,
861 Yonemochi, S. and Wang, Q.: Atmospheric HULIS and its ability to mediate the reactive oxygen
862 species (ROS): A review, *J. Environ. Sci. (China)*, 71, 13–31, doi:10.1016/j.jes.2017.12.004, 2018.

863 Wiseman, C. L. S.: Analytical methods for assessing metal bioaccessibility in airborne
864 particulate matter: A scoping review, *Anal. Chim. Acta*, 877, 9–18, doi:10.1016/j.aca.2015.01.024,
865 2015.

866 Yao, X., Fang, M., Chan, C. K., Ho, K. F. and Lee, S. C.: Characterization of dicarboxylic
867 acids in PM_{2.5} in Hong Kong, *Atmos. Environ.*, 38(7), 963–970,
868 doi:10.1016/j.atmosenv.2003.10.048, 2004.

869 Zhang, R., Wang, G., Guo, S., Zamora, M. L., Ying, Q., Lin, Y., Wang, W., Hu, M. and
870 Wang, Y.: Formation of Urban Fine Particulate Matter, *Chem. Rev.*, 115(10), 3803–3855,
871 doi:10.1021/acs.chemrev.5b00067, 2015.

872

Highlights

- Solubility and speciation of metal ions released by PM in aqueous solutions simulating fog and rainwater was investigated
- Solubility of Al, Cr, and Fe was strongly correlated to the concentrations of oxalate
- Succinate and malonate moderately affected the solubility of Cr
- Cu, Zn, Mn, Pb, and Ni were partly complexed by organic acids in solution
- Direct detection of an iron-oxalate complex was also performed in aerosol sample extracts

Declaration of interests

The authors declare that they have no known competing financial interests or personal relationships that could have appeared to influence the work reported in this paper.

The authors declare the following financial interests/personal relationships which may be considered as potential competing interests: